HHS Public Access

Author manuscript

Radiat Res. Author manuscript; available in PMC 2020 August 02.

Published in final edited form as:

Radiat Res. 2019 August ; 192(4): 367–379. doi:10.1667/RR15356.1.

12-Lipoxygenase is a Critical Mediator of Type II Pneumocyte Senescence, Macrophage Polarization and Pulmonary Fibrosis after Irradiation

Eun Joo Chung, **Jessica L. Reedy**, **Seokjoo Kwon**, **Shilpa Patil**, **Luca Valle**, **Ayla O. White**, **Deborah E. Citrin**[1]

Radiation Oncology Branch, Center for Cancer Research, National Cancer Institute, National Institutes of Health, Bethesda, Maryland 20892

Abstract

Radiation-induced pulmonary fibrosis (RIPF) is a chronic, progressive complication of therapeutic irradiation of the thorax. It has been suggested that senescence of type II pneumocytes (AECIIs), an alveolar stem cell, plays a role in the development of RIPF through loss of replicative reserve and via senescent AECII-driven release of proinflammatory and profibrotic cytokines. Within this context, we hypothesized that arachidonate 12-lipoxygenase (12-LOX) is a critical mediator of AECII senescence and RIPF. Treatment of wild-type AECIIs with 12S-hydroxyeicosateraenoic acid (12S-HETE), a downstream product of 12-LOX, was sufficient to induce senescence in a NADPH oxidase 4 (NOX4)-dependent manner. Mice deficient in 12-LOX exhibited reduced AECII senescence, pulmonary collagen accumulation and accumulation of alternatively activated (M2) macrophages after thoracic irradiation (5 × 6 Gy) compared to wild-type mice. Conditioned media from irradiated or 12S-HETE-treated primary pneumocytes contained elevated levels of IL-4 and IL-13 compared to untreated pneumocytes. Primary macrophages treated with conditioned media from irradiated AECII demonstrated preferential M2 type polarization when AECIIs were derived from wild-type mice compared to 12-LOX-deficient mice. Together, these data identified 12-LOX as a critical component of RIPF and a therapeutic target for radiation-induced lung injury.

INTRODUCTION

Nearly fifty percent of cancer patients receive radiotherapy during the course of their disease (1, 2). The development of radiation-induced pulmonary fibrosis (RIPF) is a well-recognized chronic, progressive toxicity of thoracic irradiation regardless of fractionation scheme, with few effective therapeutic strategies available. Therefore, there is a critical need to understand the mechanism involved in the development of RIPF and to identify potential targets for therapeutic intervention.

[1] Address for correspondence: Radiation Oncology Branch, Center for Cancer Research, National Cancer Institute (NCI)17), Building 10, Room B2-3500, Bethesda, MD 20892; citrind@mail.nih.gov.

Editor's note. The online version of this article (DOI: 10.1667/RR15356.1) contains supplementary information that is available to all authorized users.

Recently published studies have suggested an underlying role of alveolar epithelial injury in radiation response (3). The alveolar epithelium is composed of type 1 and type 2 pneumocytes [airway epithelial cells (AECIs and AECIIs)]. AECII maintain lung homeostasis through the production of lipid surfactants, as well as through repopulation of both AECI and AECII after injurious stimuli (4, 5). Exposure to toxic insults stimulate AECIIs to release proinflammatory cytokines and to recruit macrophages, ultimately resulting in the development of fibrosis (6–8). Furthermore, it has been demonstrated that fibrosis-inducing doses of radiation increase AECII senescence, and these senescent AECIIs stimulate fibroblast proliferation and collagen secretion (9, 10). Together, the connection between AECII response to radiation and the development of fibrosis is well established; however, the interaction of AECII senescence, macrophage polarization and fibrosis remains unclear.

We previously identified a gene expression signature of aging and senescence that was associated with radiation fibrosis in lung. One gene included in this signature, *Alox12* (*pl12-LOX* in humans and mice), encodes arachidonate 12-lipoxygenase (12-LOX), an enzyme that catalyzes peroxidation of arachidonic acid to 12S-hydroperoxyeicosatetraenoic acid (12S-HPETE), which is rapidly reduced to 12S-hydroxyeicosatetraenoic acid (12S-HETE) (11). 12S-HETE has been previously identified as a mediator in inflammatory response, including upregulation of NADPH oxidases (11,12). Importantly, the role of 12-LOX in lung fibrosis is not defined.

In this study, 12-LOX was identified as an essential signaling component in radiation-induced senescence of AECIIs in a NOX4-dependent fashion. Expression of 12-LOX in AECIIs was necessary for radiation-induced AECII secretion of IL-4 and IL-13, which were capable of polarizing macrophages to an M2 phenotype. 12-LOX deficiency was found to be protective against fibrosis in a murine model of radiation lung injury. These results demonstrate the significance of 12-LOX in RIPF and suggest a potential target for future therapeutic intervention.

MATERIALS AND METHODS

Animals and Treatments

C57/B16J (wild-type) and B6.129S2-*Alox12*$^{tm1/Fun}$/J mice (*Alox12*$^{-/-}$) were obtained from Jackson Laboratory (Bar Harbor, ME). Ten-week-old female wild-type or *Alox12*$^{-/-}$ mice received thoracic irradiation (0 Gy, 5 Gy, 17.5 Gy or 5 × 6 Gy). Irradiations were performed with mice restrained in a custom Lucite® jig with lead shielding that allows for selective thoracic irradiation with an X-RAD 320 X-ray irradiator (Precision X-ray Inc., North Branford, CT) using 2.0-mm aluminum filtration (300 kV peak) at a dose of 2.3 Gy/min. Dosimetry was verified with thermoluminescent dosimeters.

All mice were given *ad libitum* access to food and water. Lung tissue was collected from cohorts of mice at 2, 4, 8, 16 and 20 weeks postirradiation (n > 3 per condition). Lung tissue was snap frozen, inflated with neutral buffered formalin or frozen in OCT™ compound (Thermo Fisher Scientific™, Waltham, MA). Formalin-fixed lung tissue was paraffin embedded and sectioned for histologic analysis.

Isolation and Treatment of Primary AECIIs

Female wild-type or *Alox12*$^{-/-}$ mice were anesthetized 10 min after intraperitoneal injection of 12.5 μl/g body weight Heparin (Fresenius Kabi USA LLC, Lake Zurich, IL). Lungs were perfused with 10 ml of HBSS (Thermo Fisher Scientific Gibco, Waltham, MA) containing 30 m*M* HEPES (Thermo Fisher Scientific Gibco), filled with 1 ml enzyme cocktail (Elastase 3 u/ml, 0.01% DNase I,and 0.2 % Collagenase (Millipore Sigma, St. Louis, MO) in HBSS containing 30 m*M* HEPES), and incubated in 5 ml of enzyme cocktail at 37°C for 30 min. The digested tissue was carefully teased from the airways and gently swirled for 5 to 10 min. The resulting suspension was successively filtered through 100-mm and 40-mm Falcon cell strainers (Thermo Fisher Scientific), then centrifuged at 130*g* for 8 min at 4°C and resuspended in HBSS. The crude single cell suspension was applied to a Ficoll® density gradient isolation solution. Pneumocytes were collected from the layer of density 1.077–1.080, washed with HBSS and then resuspended with DMEM media containing 10% FBS and 1% antibiotic-antimycotic (100×) (Thermo Fisher Scientific). Cells were irradiated as indicated. 12S-HETE (Sigma-Aldrich® LLC, St. Louis, MO) was delivered at a concentration of 150 n*M* in DMSO for 1 or 3 days. The NOX4 inhibitor, GKT137831 (Selleck Chemicals, Houston, TX), was added 1 h prior the irradiation at a concentration of 150 n*M* in DMSO. Enriched primary pneumocyte cultures were irradiated with a single dose of 17.5 Gy, as described elsewhere (9), to avoid high rates of replicative senescence associated with multi-day fractionation regimens.

Quantitative Real-Time PCR

Total RNA was isolated from 30 mg of lung tissue with the TRIzol® reagent (Invitrogen™, Carlsbad, CA) and mechanical homogenization. After phase separation with chloroform, genomic DNA was removed with DNA eliminator columns (QIAGEN®, Valencia, CA). Total RNA was cleaned using RNAeasy spin columns (QIAGEN) according to manufacturer recommendations. Quantitative real-time PCR was performed with 0.5 μg of cDNA assayed in a 20 μl reaction volume. The reactions were incubated for 2 min at 50°C, for 10 min at 95°C for initial denaturing and followed by 50 cycles of 95°C for 15 s and 60°C for 1 min using TaqMan® Gene Expression assay primers and reagent (Thermo Fisher Scientific). Fold increase of each target was normalized to endogenous actin.

Western Blotting

Lung tissue extracts were prepared using radioimmunoprecipitation assay buffer (RIPA buffer; Pierce Chemical, Dallas, TX) containing Halt™ Protease and Phosphatase Inhibitor Cocktail (Thermo Fisher Scientific) and phosphatase inhibitors (Sigma-Aldrich), followed by measurement of protein concentrations using the Bradford method (Bio-Rad® Laboratories Inc., Hercules, CA). Equal amounts of protein were subjected to Western blot analysis, which were probed with the following primary antibodies: 12-LOX, p21, p16 (Abcam®, Cambridge, UK), NOX4 (Novus Biologicals LLC, Centennial, CO) and Actin (Millipore Sigma, Burlington, MA).

Histopathology and Histochemistry

To assess fibrosis histologically, sections of lung were deparaffinized in xylene, and rehydrated through a graded alcohol series to water. Sections were then incubated in Bouin's picric-formalin and then stained using Masson's trichrome with aniline blue as the collagen stain and Weigert's iron hematoxylin as the nuclear counterstain. Sections were dehydrated through graded alcohols to xylene, and coverslips were mounted with mounting media (Permount™; Thermo Fisher Scientific). Stained slides were examined on a Leica DM LB2 microscope (Wetzlar, Germany) and digital micrographs were captured at 40× magnification and imported into QCapture (Quantitative Imaging Corp., Surrey, Canada).

Immunohistochemistry for cell-specific markers was utilized to identify cell types in murine lungs (pro-SPC for AECII; CD68 as a pan-macrophage marker; *arginase-1* for M2 macrophages). Briefly, paraffin-embedded lung sections were deparaffinized in xylene and rehydrated through a graded alcohol series to water. Fluorescent immunohistochemical assays were performed using the specific primary antibodies (Abcam®, Cambridge, MA) against each molecule followed with compatible secondary antibodies conjugated with a fluorophore (Life Technologies, Grand Island, NY). The number of each cell type was counted on five randomly selected high-power fields (40x) in each lung (> 15 fields per group).

To visualize senescence, frozen lung sections or primary pneumocyte cultures were evaluated using a senescence-associated β-galactosidase activity assay (Abcam) according to manufacturer's instructions. To simultaneously identify AECIIs, lung tissue sections or primary cell cultures were incubated with anti-prosurfactant protein C antibody (Abcam) after β-galactosidase activity assay, and treated with compatible secondary antibody conjugated to Alexa Fluor® 594 (Life Technologies). Slides were mounted with ProLong antifade reagent containing DAPI (Life Technologies).

To assess the superoxide content of cells, 10 μ*M* of dihydroethidium (DHE; Thermo Fisher Molecular Probes, Waltham, MA) was added to enriched primary AECIIs from the lungs of wild-type and *Alox12*$^{-/-}$ mice at 24 h after 17.5 Gy irradiation. After 30 min incubation with DHE at 37°C in a CO_2 incubator, the cells were washed twice with cold phosphate buffered saline (PBS). Red fluorescence was recorded using the EVOS® cell imaging system (Thermo Fisher Scientific), and its intensity was measured in 50 cells using ImageJ Software (National Institutes of Health, Bethesda, MD; open source: https://imagej.nih.gov/ij/docs/index.html).

ELISA

Lung tissue was homogenized in RIPA buffer containing protease inhibitors. Soluble proteins were separated from insoluble material by centrifugation (16,000*g*, 10 min), and the total protein count of the resulting supernatant was determined using the Bradford method (BioRad). The supernatant was then subjected to ELISA to determine the concentrations of 12S-LOX using an ELISA kit (MyBioSource, San Diego, CA). The amount of IL-4 and IL-13 was assessed in culture supernatants from primary AECII cells after different

treatments as indicated using DuoSet® ELISA assay kits (R&D Systems™, Minneapolis, MN).

Hydroxyproline Assay

The right-side lung (n ≥ 3 mice per cohort) was weighed at the time of collection, mechanically homogenized and snap frozen. Pulmonary hydroxyproline content was measured after hydrolysis of a known weight of lung tissue in 1 ml of 6 N HCl at 1l0°C for 18 h. Hydrosylate was analyzed using the BioVision Hydroxyproline Assay Kit (Milpitas, CA) according to manufacturer instructions. The increase in pulmonary hydroxyproline per mouse was calculated based on total lung weight and expressed as ig in the lung.

Macrophage Polarization

Bone marrow-derived monocytes (BMDM) were pre-differentiated into M0 macrophages by culture for 6 days in RPMI/10% FCS supplemented with 20 ng/ml of M-CSF (PeproTech®, Rocky Hill, NJ). M0 macrophages prepared from bone marrow were incubated with complete media containing 50% culture supernatants collected from differently treated primary AECII cells. For macrophage stimulation assays, M0 macrophages were prepared from wild-type or *Alox12*$^{-/-}$ mice and treated with 1 ng/mL LPS (Peprotech, Rocky Hill, NJ), 10 ng/ml IL-4 (Sigma-Aldrich, St. Louis, MO), 10 ng/mL IL-13 (Sigma-Aldrich, St. Louis, MO) or PBS (Thermo Fisher Scientific Gibco). After 24 h, total RNA was isolated from each macrophage group and analyzed with quantitative real time PCR for *Arg-1* and *iNOS* using TaqMan® Gene Expression assay primers and reagent (Thermo Fisher Scientific). Fold increase of each target was normalized to endogenous actin.

Statistical Analysis

For *in vitro* studies, comparisons between conditions were evaluated using one-way analysis of variance (ANOVA) with Tukey's correction for multiple comparisons. A *P* value of less than 0.05 was considered statistically significant. *In vitro* studies were performed in duplicate and validated in three separate experiments. For *in vivo* studies, comparisons between conditions were evaluated with two-way ANOVA with Tukey's correction for multiple comparisons.

RESULTS

12-LOX Expression is Increased in Murine Lung after Fibrosis-Inducing Doses of Radiation

We previously identified an aging- and senescence-related pattern of gene expression in radiation-induced murine lung fibrosis (9). Increased expression of *Alox12* after *in vivo* 17.5 Gy irradiation, as assessed using cDNA microarray, contributed to this published signature. To confirm that two previously reported fibrosis-evoking dose regimens of radiation increase the expression of *Alox12* RNA, wild-type mice received 0 Gy, 5 Gy, 17.5 Gy and 5 × 6 Gy thoracic irradiation and *Alox12* RNA expression was evaluated across multiple timepoints. Mice that received a fibrogenic dose of radiation (17.5 Gy, 5 × 6 Gy) had significant increases in *Alox12* RNA expression (Fig. 1A) in the first 8 weeks postirradiation. In contrast, mice receiving either no radiation or a 5 Gy single dose had no significant changes from baseline in *Alox12* expression through the 30-week timepoint. ELISA (Fig. 1B) was

used to determine the effects of radiation on 12-LOX protein expression. Consistent with *Alox12* gene expression, 12-LOX protein expression was similar in the lung tissue at all timepoints in the nonirradiated mice and the mice receiving 5 Gy thoracic irradiation. Lung tissue from mice irradiated at 17.5 Gy had a significant increase by week 8. Furthermore, mice receiving the more rapidly lethal 5 × 6 Gy thoracic irradiation (9) demonstrated a significant increase in *Alox12* RNA expression as early as week 2 postirradiation. This pattern was mirrored in 12-LOX protein levels assessed using Western blotting in whole lung tissue lysates (Fig. 1C).

To identify the population of cells in lung tissue responsible for the increase in 12-LOX expression after irradiation, specific cell types were isolated from irradiated murine lung tissue (5 × 6 Gy) and analyzed using Western blotting for 12-LOX (Fig. 1D). Fibrosis-inducing doses of radiation increased 12-LOX expression in AECIIs, but not in AECIs, macrophages or the remaining cell types.

12S-HETE Induces Senescence in AECII Through Increase of NOX4 and p21 Expression

A growing body of evidence implicates AECII senescence in the development of fibrosis (9,10,14). Established senescence biomarkers, such as p16, p21 and senescence-associated β-galactosidase activity (SA-β-gal), have been observed to accumulate in fibrotic lung tissue. To determine the importance of 12-LOX in AECII senescence, enriched AECII primary pneumocyte cultures were either irradiated at 17.5 Gy or administered 12S-HETE, the active product of arachidonic acid oxidation by 12-LOX. Both radiation and 12S-HETE were sufficient for increasing SA-β-gal activity in AECIIs compared to nonirradiated AECIIs (Fig. 2A). These data suggest that 12-LOX metabolites are involved in the induction of senescence.

An increase in NADPH oxidase (NOX) expression has been associated with the development of senescence, and inhibition of NADPH oxidases has been demonstrated to reduce AECII senescence *in vitro* and *in vivo* after irradiation (9, 15). Indeed, expression of NOX4 and p21, but not p16, was increased in AECIIs after 17.5 Gy irradiation or 12S-HETE treatment (Fig. 2B). To determine if NOX activity was required for 12S-HETE-induced AECII senescence, AECIIs were irradiated at 17.5 Gy or administered 12S-HETE in the presence of GKT137831, an inhibitor of NADPH oxidases. Both radiation and 12S-HETE significantly increased the senescent AECII population (Fig. 2C). Treatment of AECIIs with GKT137831 was capable of attenuating both radiation- and 12S-HETE-induced senescence (Fig. 2C). Together, these data suggest that 12-LOX metabolites and radiation promote AECII senescence through increases of NOX4 and p21. To confirm a role of 12-LOX in superoxide production after irradiation, primary pneumocytes generated from wild-type and *Alox12*$^{-/-}$ mice received 17.5 Gy irradiation. Radiation exposure resulted in increased DHE oxidation in wild-type AECIIs, whereas AECIIs deficient in 12-LOX showed no significant change in DHE oxidation after irradiation (Supplementary Fig. S1; https://doi.org/10.1667/RR15356.1.S1).

Deficiency of 12-LOX Attenuates Radiation-Induced Fibrosis and M2 Macrophage Accumulation

To confirm a causative role of 12-LOX signaling in the development of radiation-induced senescence and fibrosis, wild-type and *Alox12*$^{-/-}$ mice received either 0 Gy or 5 × 6 Gy thoracic irradiation. The fractionated 5 × 6 Gy regimen was utilized for studies in genetically deficient mice, since it accelerates the fibrotic process (9), reduces dermatitis compared to a single fraction, and has been shown to be biologically similar in regard to 12-LOX expression (Fig. 1). At 20 weeks postirradiation, lung tissue was analyzed for collagen deposition (Fig. 3A). Wild-type irradiated mice had a significant increase in fibrotic foci (Fig. 3A and B) and hydroxyproline content compared to nonirradiated controls (Fig. 3C). Deficiency of 12-LOX significantly reduced radiation-induced accumulation of fibrotic foci and increase in hydroxyproline content. As expected, irradiated wild-type mice had a significant increase in the proportion of senescent AECIIs compared to nonirradiated controls (Fig. 3D). In contrast, in *Alox12*$^{-/-}$ mice, the proportion of AECIIs with SA-β-gal activity after irradiation was significantly reduced compared to that observed in irradiated wild-type lung tissue. Together, these data confirm a role of 12-LOX in the accumulation of senescent AECIIs after irradiation and in the progression of radiation-induced fibrosis.

Alternatively-activated macrophages play a critical role in radiation fibrosis (16, 17). Exposure of the lung to fibrosis-evoking radiation doses results in a slow but progressive accumulation of macrophages, with histologic evidence of macrophage accumulation beginning at 8 weeks (18) and increasing over time (19). To determine the effect of 12-LOX deficiency on macrophage accumulation and polarization after irradiation *in vivo,* macrophages were visualized in lung tissue at 20 weeks after 5 × 6 Gy fractions using immunohistochemistry. Macrophage accumulation was studied at 20 weeks postirradiation because it occurs just prior to mice succumbing to lung injury, is the peak of macrophage accumulation and is therefore relevant in determining if changes set forth earlier in the disease course can affect the long-term inflammatory environment. Macrophage accumulation (CD68^{+} cells) was significantly increased in irradiated wild-type mice compared to wildtype controls (Fig. 3). No significant difference in macrophage accumulation in lung tissue was observed in *Alox12*$^{-/-}$ mice after thoracic irradiation. A more pronounced accumulation of M2 polarized macrophages (arginase-1^{+}) was observed after irradiation in wild-type mice (Fig. 3F). In contrast, accumulation of M2 macrophages in lung tissue after irradiation in *Alox12*$^{-/-}$ mice was not elevated compared to nonirradiated controls, suggesting that 12-LOX plays a crucial role in the polarization of M2 macrophages after irradiation.

12-LOX Stimulates AECII Production of IL-4 and IL-13

Type 2 cytokines, such as IL-4 and IL-13, can stimulate macrophage polarization to an alternatively activated phenotype (20). Of note, IL-13 has been shown to play a critical role in radiation lung injury through recruitment and polarization of alternatively activated macrophages and increased expression of fibrosis-associated genes (16, 17). To determine if irradiated AECIIs contribute to this phenomenon, enriched AECII primary pneumocyte cultures irradiated at 17.5 Gy, and mRNA expression for several cytokines known to be important in fibrosis, inflammation and macrophage polarization were analyzed at days 1

and 3 postirradiation by qPCR analysis. At day 1, exposure to 17.5 Gy significantly increased the expression of *IL-4* compared to control (Fig. 4A). By day 3, the expression of *IL-13, Alox12* and *IGF1* were significantly increased after 17.5 Gy irradiation compared to control. A strikingly similar pattern of gene expression was noted in enriched primary AECII cultures treated with 12S-HETE, with early induction of IL-4 and increased expression of IL-13 by day 3 (Fig. 4B). Increased expression of IL-4 and IL-13 after irradiation or 12S-HETE were confirmed at the protein level in conditioned media from identically treated AECII cultures (Fig. 4C and D). Together, these data suggest that 12-LOX stimulates AECII secretion of cytokines that may contribute to macrophage polarization to an M2 phenotype.

12-LOX Participates in AECII-Mediated Macrophage Polarization

Having identified that AECIIs secrete cytokines that are known to induce alternative activation of macrophages, further experiments were undertaken to determine if cytokines elaborated from primary AECII cultures after irradiation or 12S-HETE treatment could effectively polarize macrophages. Primary AECIIs enriched from wild-type and *Alox12*$^{-/-}$ mice were 0 Gy or 17.5 Gy irradiated in culture (Fig. 5A). Three days postirradiation, both conditioned media and AECII RNA were collected. *IL-13* RNA was significantly increased by after 17.5 Gy irradiation in wild-type AECIIs, but not in *Alox12*$^{-/-}$ AECIIs (Fig. 5B), recapitulating previous results obtained with 12S-HETE treatment (Fig. 4B–D).

To determine if irradiated AECIIs have the capacity to drive macrophage polarization and to identify the role of 12-LOX in this effect, BMDM isolated from wild-type mice were cultured with the AECII-conditioned media. Macrophages treated with conditioned media from wild-type AECIIs irradiated at 17.5 Gy displayed a significant increase in *Arg-1* mRNA (Fig. 5C), a marker of alternative activation. This effect was not observed when conditioned media from 17.5 Gy irradiated *Alox12*$^{-/-}$ AECIIs was applied to BMDM, suggesting that 12-LOX activity is critical to this effect. In contrast, conditioned media from 17.5 Gy irradiated wild-type AECIIs increased the expression of *iNOS,* a marker of classical macrophage activation (M1), but the increase in expression was not significant compared to application of conditioned media from nonirradiated wild-type AECIIs. Furthermore, *iNOS* expression was significantly increased in BMDM treated with conditioned media from *Alox12*$^{-/-}$ AECIIs relative to nonirradiated wild-type AECIIs (Fig. 5D). Together, these data support the hypothesis that 12-LOX mediates IL-13 production by irradiated AECIIs, which are capable of altering macrophage polarization.

12-LOX-Deficient Macrophages have a Reduced Response to M2 Polarizing Stimuli

Previously published studies have demonstrated the importance of other downstream products of lipoxygenase metabolism of arachidonic acid, such as 15-HETE, in macrophage polarization in allergic conditions (21–25). It is therefore conceivable that a reduction in the accumulation of M2 macrophages in irradiated lung could also be affected by deficiency of a lipoxygenase in macrophages in the *Alox12*$^{-/-}$ mice. To determine if the deficiency of 12-LOX in *Alox12*$^{-/-}$ macrophages altered the capacity for polarization after irradiation, BMDM from wild-type and *Alox12*$^{-/-}$ mice were treated with vehicle, LPS or IL-13. As expected, IL-13 treatment increased the expression of *Arg-1* and LPS treatment increased

the expression of *iNOS* relative to vehicle control in BMDM from wild-type mice (Fig. 5E and F). BMDM derived from *Alox12*$^{-/-}$ mice had a blunted response to IL-13 compared to wild-type mice, which was partially rescued with the addition of 12S-HETE to the culture media. Importantly, the treatment of BMDM derived from wild-type or *Alox12*$^{-/-}$ mice with 12S-HETE, in the absence of IL-13 or LPS, did not affect the expression *Arg-1* or *iNOS,* suggesting that 12S-HETE does not independently alter macrophage polarization but may enhance the effects of IL-13.

DISCUSSION

Radiation-induced fibrosis is considered refractory to most treatments and exhibits a chronic, progressive course. Indeed, there are no FDA-approved pharmacologic agents for treatment of radiation-induced fibrosis in any organ. The pathological mechanism of fibrosis can vary by the initiating insult and the organ in which the insult occurs. In lung fibrosis, the pathological mechanism is associated with elaboration of pro-fibrotic and immunomodulatory cytokines, pneumocyte senescence and death, chronic type 2 inflammation and collagen accumulation (9, 26–28). Within this context, prior work demonstrated a significant increase in the expression of *Alox12,* a gene that encodes 12-lipoxygenase (12-LOX), in lung tissue exposed to fibrogenic doses of radiation (9); however, the involvement of lipoxygenases in lung fibrosis remains largely unexplored.

Lipoxygenases (LOX) catalyze the formation of hydro-peroxyl eicosatetraenoic acids from arachidonic acid, which can function as signaling molecules that influence numerous physiologic processes. Six LOX isoforms are derived from each corresponding ALOX gene in humans (*ALOX15, ALOX15B, ALOX12, ALOX12B, ALOXE3* and *ALOX5*), and in mice (*Alox15, Alox15b, Alox12, Alox12b, Aloxe3* and *Alox5*) (29, 30). These isoforms are distinguished by their differential organ expression patterns and their specific products. 12-LOX (encoded by *ALOX12* in humans and *Alox12* in mice) has been primarily investigated in leukocyte and myeloid lineage cells (31–33); however, 12-LOX expression has also been identified in human and murine epithelium (34, 35). Polymorphisms in *ALOX12* are associated with an assortment of health conditions, including cancers, neurological disorders and hypertension (36–39), supporting the critical role of 12-LOX in maintaining homeostasis.

In this study, we identify 12-LOX, a known marker of aging and senescence (40), as a mediator of radiation-induced lung injury, while highlighting potential therapeutic implications. 12-LOX catalyzes arachidonic acid to 12S-HPETE, which is rapidly reduced to 12S-HETE, due to intrinsic glutathione peroxidase activity (41). A critical finding in this work is the capacity of 12S-HETE to induce NADPH-oxidase-dependent senescence in AECIIs. Exposure of murine lung tissue to fibrogenic doses was confirmed to increase *Alox12* expression and that of the protein it encodes, 12-LOX, as early as two weeks postirradiation. This increased expression of 12-LOX was identified only in AECIIs, with minimal increase in other cell types, consistent with senescence-associated expression of 12-LOX and prior findings, reported elsewhere, of senescence preferentially occurring in AECIIs after irradiation (9). In addition to the known signaling roles of 12S-HETE, these findings suggest a mechanism by which senescent AECIIs can induce secondary senescence,

namely via paracrine interactions. Furthermore, the critical role of NADPH oxidases in AECII senescence and lung fibrosis after irradiation have previously been demonstrated (9); however, the intermediaries involved in increased AECII NOX expression have not been elucidated. An understanding of the pathways leading to increased NOX activity and superoxide elaboration after irradiation in AECIIs may identify therapeutic targets. Previously published work has suggested 5-HETE, a metabolite of 5-LOX, may have the capacity to induce a stasis-like phenotype in fibroblasts in a p53-dependent mechanism, although downstream intermediaries of 12-LOX and the contribution of NADPH-oxidase have not been explored in this context (13).

Based on previously published work linking 12S-HETE to allergic and autoimmune diseases characterized by type 2 inflammation (21–25), we hypothesized that 12-LOX plays a critical role in the initiation and maintenance of macrophage accumulation and polarization in irradiated lung. Herein, we sought to characterize changes in the inflammatory milieu of the irradiated lung in the context of 12-LOX deficiency. Accumulation of predominantly alternatively-activated macrophages, characterized by expression of *arginase-1*, was readily evident in the alveolar space after irradiation in wild-type mice, but was substantially reduced in the absence of 12-LOX. These findings strongly suggest that 12-LOX and its lipid mediators may contribute to the presence of type 2 polarized inflammation in lung after irradiation.

IL-13 has been demonstrated to play a critical role in conditions dominated by type 2 inflammation such as parasite-induced (42, 43) and radiation-induced fibrosis (16). In contrast, the type 2 cytokine IL-4 has been shown to alter macrophage accumulation after irradiation, but has no effect on the progression of radiation-induced lung fibrosis (17). In this study, the decrease in *arginase-1*-positive macrophages in the lungs of irradiated 12-LOX-deficient mice compared to lungs of irradiated wild-type mice suggested that 12-LOX deficiency may affect cytokines involved in the type 2 inflammatory response, such as IL-4 and IL-13. Because of the known pathogenic role of IL-13 in fibrosis, we chose to focus on IL-13. Indeed, the expression of IL-13 was increased in AECIIs after irradiation or 12S-HETE, and exposure of macrophages to the factors secreted by irradiated AECIIs was sufficient to increase *arginase-1* expression, a phenomenon that was reduced in the absence of 12-LOX.

In contrast to our findings that 12-LOX contributes to radiation-induced fibrosis and maintenance of type 2 inflammation, it has previously been reported that delivery of 12S/15S-HETE to the airways of mice attenuated allergic airway inflammation (44). Two additional published studies have suggested that deficiency of 12/15-LOX encoded by the *Alox15* gene in mice attenuates airway inflammation in asthma models (45, 46). Although radiation lung injury and allergic airway inflammation share similarities, such as an inflammatory environment dominated by type 2 cytokines, it is important to note that asthma models primarily reflect airway inflammation, whereas radiation fibrosis largely spares the airways while resulting in dense fibrosis in the alveolar space. Thus, it is conceivable that the pathways and inflammatory mediators of biological relevance may differ in these distinct pulmonary microenvironments. Furthermore, 12/15-LOX is a leukocyte-type isoform of LOXs which is expressed in different cell types compared to 12-LOX, a platelet-type LOX.

Indeed, published studies in airway inflammation have suggested a lack of 12-LOX expression in bronchial airway epithelial cells (47), in contrast to the abundant expression in pneumocytes observed in this work.

Prior work has demonstrated that IL-4 and IL-13 upregulate leukocyte-type 12/15-LOX activity in macrophages (44, 48) in a STAT6-dependent fashion (48). In the allergic airway inflammation model, Ym1/2 lectin, a product of type 2 inflammation secreted in response to IL-13, induced the expression of 12-LOX in dendritic cells (44). Furthermore, exposure of dendritic cells to 12S-HETE resulted in reduced expression of IL-13. These previously published findings coupled with the current work demonstrating 12S-HETE-increased IL-13 expression in AECIIs further support the notion that the effects of 12S-HETE are cell type and context specific.

AECIIs are a subset of pulmonary epithelial cells that function as an alveolar stem cell and as a major secretory component of the pulmonary epithelia via elaboration of surfactant. AECII depletion has been implicated as a causal factor in fibrotic lung pathologies (6, 49). In contrast, alveolar macrophages occupy a unique niche within the alveolus and are known to exhibit a high-degree phenotypic plasticity (50). An important component of alveolar macrophage homeostasis is moderated via cell-cell interactions and soluble mediators from surrounding tissue, such as cytokines, CD200/CD200R, triggering receptor expressed by myeloid cells, and Toll-like receptors (50–54). Indeed, many soluble factors in healthy lung function as a suppressive stimulus for alveolar macrophages, ensuring homeostasis. However, the contribution of monocyte/ epithelial interactions in the context of radiation lung injury and the type 2 inflammatory program remains largely unexplored. A novel finding in this work is the capacity of products secreted from AECIIs to influence the polarization of macrophages in a 12-LOX-dependent manner. We demonstrate that AECII cells, exposed to damaging stimuli such as radiation, elaborate factors capable of altering the phenotype of macrophages, including IL-4 and IL-13. These results support previously reported findings that irradiated alveolar macrophages exhibit a type 2 polarized phenotype (16). When the irradiated AECIIs are derived from 12-LOX-deficient mice, IL-13 expression is not induced by radiation and macrophages cultured with AECII conditioned media do not exhibit markers of alternative activation. Coupled with the observation that the lung tissue from irradiated 12-LOX-deficient mice exhibits attenuated accumulation of *arginase-1* expressing macrophages, these data suggest that irradiated AECIIs contribute to alveolar macrophage polarization via secretion of soluble factors in a 12-LOX and NADPH oxidase-dependent fashion.

The mice used for studies were globally genetically deficient in 12-LOX. This genetically modified mouse model provides greater confidence in specificity of these findings to 12-LOX than would be obtained with pharmacologic inhibitors of lipoxygenases, which are known to have off-target GABAergic and metabolic targets (55, 56). As a result, future studies using site-specific recombinase technology may be beneficial in determining the relative impact of 12-LOX deficiency in various cell-specific lineages *in vivo,* validating the co-culture experiments using cell lineages derived from wild-type and genetically-deficient mice presented herein.

CONCLUSION

In this study, the importance of AECII senescence in radiation-induced lung fibrosis and the capacity to mitigate radiation lung injury by preventing AECII senescence have been established. Radiation-induced 12-LOX expression mediates RIPF through increases in NOX4- and p21-driven AECII senescence. Senescent AECII elaborate type 2 polarizing cytokines IL-4 and IL-13, which are capable of altering macrophage phenotype. Together, these data highlight the importance of macrophage-epithelial interactions in the context of lung injury and chronic inflammation and have identified 12-LOX as a critical component of RIPF as well as a potential therapeutic target for radiation lung injury.

Supplementary Material

Refer to Web version on PubMed Central for supplementary material.

ACKNOWLEDGMENT

This research was supported by the NIH Intramural Research Program, National Cancer Institute Center for Cancer Research.

REFERENCES

1. Begg AC, Stewart FA, Vens C Strategies to improve radiotherapy with targeted drugs. Nat Rev Cancer 2011; 11:239–53. [PubMed: 21430696]
2. Delaney G, Jacob S, Featherstone C, Barton M The role of radiotherapy in cancer treatment: estimating optimal utilization from a review of evidence-based clinical guidelines. Cancer 2005; 104:1129–37. [PubMed: 16080176]
3. Almeida C, Nagarajan D, Tian J, Leal SW, Wheeler K, Munley M, et al. The role of alveolar epithelium in radiation-induced lung injury. PLoS One 2013; 8:e53628.
4. Fehrenbach H Alveolar epithelial type II cell: defender of the alveolus revisited. Respir Res 2001; 2:33–46. [PubMed: 11686863]
5. Evans MJ, Cabral LJ, Stephens RJ, Freeman G Transformation of alveolar type 2 cells to type 1 cells following exposure to NO2. Exp Mol Pathol 1975; 22:142–50. [PubMed: 163758]
6. Sisson TH, Mendez M, Choi K, Subbotina N, Courey A, Cunningham A, et al. Targeted injury of type II alveolar epithelial cells induces pulmonary fibrosis. Am J Respir Crit Care Med 2010; 181:254–63. [PubMed: 19850947]
7. Osterholzer JJ, Olszewski MA, Murdock BJ, Chen GH, Erb-Downward JR, Subbotina N, et al. Implicating exudate macrophages and Ly-6C(high) monocytes in CCR2-dependent lung fibrosis following gene-targeted alveolar injury. J Immunol 2013; 190:3447–57. [PubMed: 23467934]
8. Byrne AJ, Maher TM, Lloyd CM. Pulmonary Macrophages: A new therapeutic pathway in fibrosing lung disease? Trends Mol Med 2016; 22:303–16. [PubMed: 26979628]
9. Citrin DE, Shankavaram U, Horton JA, Shield W 3rd, Zhao S, Asano H, et al. Role of type II pneumocyte senescence in radiation-induced lung fibrosis. J Natl Cancer Inst 2013; 105:1474–84. [PubMed: 24052614]
10. Schafer MJ, White TA, Iijima K, Haak AJ, Ligresti G, Atkinson EJ, et al. Cellular senescence mediates fibrotic pulmonary disease. Nat Commun 2017; 8:14532. [PubMed: 28230051]
11. Cheresh P, Kim SJ, Tulasiram S, Kamp DW. Oxidative stress and pulmonary fibrosis. Biochim Biophys Acta 2013; 1832:1028–40. [PubMed: 23219955]
12. Zhang XJ, Cheng X, Yan ZZ, Fang J, Wang X, Wang W, et al. An ALOX12–12-HETE-GPR31 signaling axis is a key mediator of hepatic ischemia-reperfusion injury. Nat Med 2018; 24:73–83. [PubMed: 29227475]

13. Catalano A, Rodilossi S, Caprari P, Coppola V, Procopio A 5-Lipoxygenase regulates senescence-like growth arrest by promoting ROS-dependent p53 activation. EMBO J 2005; 24:170–9. [PubMed: 15616590]
14. Waters DW, Blokland KEC, Pathinayake PS, Burgess JK, Mutsaers SE, Prele CM, et al. Fibroblast senescence in the pathology of idiopathic pulmonary fibrosis. Am J Physiol Lung Cell Mol Physiol 2018; 315:L162–72. [PubMed: 29696986]
15. Weyemi U, Lagente-Chevallier O, Boufraqech M, Prenois F, Courtin F, Caillou B, et al. ROS-generating NADPH oxidase NOX4 is a critical mediator in oncogenic H-Ras-induced DNA damage and subsequent senescence. Oncogene 2011; 31:1117. [PubMed: 21841825]
16. Chung SI, Horton JA, Ramalingam TR, White AO, Chung EJ, Hudak KE, et al. IL-13 is a therapeutic target in radiation lung injury. Sci Rep 2016; 6:39714. [PubMed: 28004808]
17. Groves AM, Johnston CJ, Misra RS, Williams JP, Finkelstein JN. Effects of IL-4 on pulmonary fibrosis and the accumulation and phenotype of macrophage subpopulations following thoracic irradiation. Int J Radiat Biol 2016; 92:754–65. [PubMed: 27539247]
18. Groves AM, Johnston CJ, Misra RS, Williams JP, Finkelstein JN. Whole-lung irradiation results in pulmonary macrophage alterations that are subpopulation and strain specific. Radiat Res 2015; 184:639–49. [PubMed: 26632857]
19. Chung EJ, Hudak K, Horton JA, White A, Scroggins BT, Vaswani S, et al. Transforming growth factor alpha is a critical mediator of radiation lung injury. Radiat Res 2014; 182:350–62. [PubMed: 25117621]
20. Zhou D, Huang C, Lin Z, Zhan S, Kong L, Fang C, et al. Macrophage polarization and function with emphasis on the evolving roles of coordinated regulation of cellular signaling pathways. Cell Signal 2014; 26:192–7. [PubMed: 24219909]
21. Voorhees JJ. Leukotrienes and other lipoxygenase products in the pathogenesis and therapy of psoriasis and other dermatoses. Arch Dermatol 1983; 119:541–7. [PubMed: 6305285]
22. Wollard PM, Cunnigham FM, Murphy GM, Camp RD, Derm FF, Greaves MW. A comparison of the proinflammatory effects of 12(R)- and 12(S)-hydroxy-5,8,10,14-eicosatetraenoic acid in human skin. Prostaglandins 1989; 38:465–71. [PubMed: 2813813]
23. Samala N, Tersey SA, Chalasani N, Anderson RM, Mirmira RG. Molecular mechanisms of nonalcoholic fatty liver disease: Potential role for 12-lipoxygenase. J Diabetes Complications 2017; 31:1630–7. [PubMed: 28886991]
24. Xu J, Zhang Y, Xiao Y, Ma S, Liu Q, Dang S, et al. Inhibition of 12/15-lipoxygenase by baicalein induces microglia PPARbeta/delta: a potential therapeutic role for CNS autoimmune disease. Cell Death Dis 2013; 4:e569.
25. Wu GS, Sevanian A, Rao NA. Detection of retinal lipid hydroperoxides in experimental uveitis. Free Radic Biol Med 1992; 12:19–27. [PubMed: 1537568]
26. Trott KR, Herrmann T, Kasper M Target cells in radiation pneumopathy. Int J Radiat Oncol Biol Phys 2004; 58:463–9. [PubMed: 14751516]
27. Rube CE, Uthe D, Schmid KW, Richter KD, Wessel J, Schuck A, et al. Dose-dependent induction of transforming growth factor beta (TGF-beta) in the lung tissue of fibrosis-prone mice after thoracic irradiation. Int J Radiat Oncol Biol Phys 2000; 47:1033–42. [PubMed: 10863076]
28. Rube CE, Wilfert F, Palm J, Konig J, Burdak-Rothkamm S, Liu L, et al. Irradiation induces a biphasic expression of pro-inflammatory cytokines in the lung. Strahlenther Onkol 2004; 180:442–8. [PubMed: 15241532]
29. Kuhn H, Banthiya S, van Leyen K Mammalian lipoxygenases and their biological relevance. Biochim Biophys Acta 2015; 1851:308–30. [PubMed: 25316652]
30. Mashima R, Okuyama T The role of lipoxygenases in pathophysiology; new insights and future perspectives. Redox Biol 2015: 6:297–310. [PubMed: 26298204]
31. Brune B, Ullrich V 12-hydroperoxyeicosatetraenoic acid inhibits main platelet functions by activation of soluble guanylate cyclase. Mol Pharmacol 1991; 39:671–8. [PubMed: 1674588]
32. Ikei KN, Yeung J, Apopa PL, Ceja J, Vesci J, Holman TR, et al. Investigations of human platelet-type 12-lipoxygenase: role of lipoxygenase products in platelet activation. J Lipid Res 2012; 53:2546–59. [PubMed: 22984144]

33. Yeung J, Holinstat M 12-lipoxygenase: a potential target for novel anti-platelet therapeutics. Cardiovasc Hematol Agents Med Chem 2011; 9:154–64. [PubMed: 21838667]
34. Nigam S, Kumar GS, Sutherland M, Schewe T, Ikawa H, Yamasaki Y, et al. Metabolic suppression of platelet-type 12-lipoxygenase in human uterine cervix with invasive carcinoma. Int J Cancer 1999; 82:827–31. [PubMed: 10446449]
35. Virmani J, Johnson EN, Klein-Szanto AJ, Funk CD. Role of 'platelet-type' 12-lipoxygenase in skin carcinogenesis. Cancer Lett 2001; 162:161–5. [PubMed: 11146221]
36. Fridman C, Ojopi EP, Gregorio SP, Ikenaga EH, Moreno DH, Demetrio FN, et al. Association of a new polymorphism in ALOX12 gene with bipolar disorder. Eur Arch Psychiatry Clin Neurosci 2003; 253:40–3. [PubMed: 12664313]
37. Gonzalez-Nunez D, Claria J, Rivera F, Poch E Increased levels of 12(S)-HETE in patients with essential hypertension. Hypertension 2001; 37:334–8. [PubMed: 11230294]
38. Prasad VV, Kolli P, Moganti D Association of a functional polymorphism (Gln261Arg) in 12-lipoxygenase with breast cancer. Exp Ther Med 2011; 2:317–23. [PubMed: 22977504]
39. Quintana LF, Guzman B, Collado S, Claria J, Poch E A coding polymorphism in the 12-lipoxygenase gene is associated to essential hypertension and urinary 12(S)-HETE. Kidney Int 2006; 69:526–30. [PubMed: 16514435]
40. Coppe JP, Desprez PY, Krtolica A, Campisi J The senescence-associated secretory phenotype: the dark side of tumor suppression. Annu Rev Pathol 2010; 5:99–118. [PubMed: 20078217]
41. Bryant RW, Simon TC, Bailey JM. Role of glutathione peroxidase and hexose monophosphate shunt in the platelet lipoxygenase pathway. J Biol Chem 1982; 257:14937–43. [PubMed: 6816802]
42. Chiaramonte MG, Schopf LR, Neben TY, Cheever AW, Donaldson DD, Wynn TA. IL-13 is a key regulatory cytokine for Th2 cell-mediated pulmonary granuloma formation and IgE responses induced by Schistosoma mansoni eggs. J Immunol 1999; 162:920–30. [PubMed: 9916716]
43. Zhu Z, Homer RJ, Wang Z, Chen Q, Geba GP, Wang J, et al. Pulmonary expression of interleukin-13 causes inflammation, mucus hypersecretion, subepithelial fibrosis, physiologic abnormalities, and eotaxin production. J Clin Invest 1999; 103:779–88. [PubMed: 10079098]
44. Cai Y, Kumar RK, Zhou J, Foster PS, Webb DC. Ym1/2 promotes Th2 cytokine expression by inhibiting 12/15(S)-lipoxygenase: identification of a novel pathway for regulating allergic inflammation. J Immunol 2009; 182:5393–9. [PubMed: 19380786]
45. Hajek AR, Lindley AR, Favoreto S Jr., Carter R, Schleimer RP, Kuperman DA. 12/15-Lipoxygenase deficiency protects mice from allergic airways inflammation and increases secretory IgA levels. Allergy Clin Immunol 2008; 122:633–9.e3.
46. Andersson CK, Claesson HE, Rydell-Tormanen K, Swedmark S, Hallgren A, Erjefalt JS. Mice lacking 12/15-lipoxygenase have attenuated airway allergic inflammation and remodeling. Am J Respir Cell Mol Biol 2008; 39:648–56. [PubMed: 18511709]
47. Mabalirajan U, Rehman R, Ahmad T, Kumar S, Leishangthem GD, Singh S, et al. 12/15-lipoxygenase expressed in non-epithelial cells causes airway epithelial injury in asthma. Sci Rep 2013: 3:1540. [PubMed: 23528921]
48. Heydeck D, Thomas L, Schnurr K, Trebus F, Thierfelder WE, Ihle JN, et al. Interleukin-4 and −13 induce upregulation of the murine macrophage 12/15-lipoxygenase activity: evidence for the involvement of transcription factor STAT6. Blood 1998; 92:2503–10. [PubMed: 9746791]
49. Barbas-Filho JV, Ferreira MA, Sesso A, Kairalla RA, Carvalho CR, Capelozzi VL. Evidence of type II pneumocyte apoptosis in the pathogenesis of idiopathic pulmonary fibrosis (IFP)/usual interstitial pneumonia (UIP). J Clin Pathol 2001; 54:132–8. [PubMed: 11215282]
50. Hussell T, Bell TJ. Alveolar macrophages: plasticity in a tissue-specific context. Nat Rev Immunol 2014; 14:81–93. [PubMed: 24445666]
51. Fernandez S, Jose P, Avdiushko MG, Kaplan AM, Cohen DA. Inhibition of IL-10 receptor function in alveolar macrophages by Toll-like receptor agonists. J Immunol 2004; 172:2613–20. [PubMed: 14764735]
52. Gao X, Dong Y, Liu Z, Niu B Silencing of triggering receptor expressed on myeloid cells-2 enhances the inflammatory responses of alveolar macrophages to lipopolysaccharide. Mol Med Rep 2013; 7:921–6. [PubMed: 23314916]

53. Mayer AK, Bartz H, Fey F, Schmidt LM, Dalpke AH. Airway epithelial cells modify immune responses by inducing an anti-inflammatory microenvironment. Eur J Immunol 2008; 38:1689–99. [PubMed: 18421791]

54. Snelgrove RJ, Goulding J, Didierlaurent AM, Lyonga D, Vekaria S, Edwards L, et al. A critical function for CD200 in lung immune homeostasis and the severity of influenza infection. Nat Immunol 2008; 9:1074–83. [PubMed: 18660812]

55. Si D, Wang Y, Zhou YH, Guo Y, Wang J, Zhou H, et al. Mechanism of CYP2C9 inhibition by flavones and flavonols. Drug Metab Dispos 2009; 37:629–34. [PubMed: 19074529]

56. Wang F, Xu Z, Ren L, Tsang SY, Xue H. GABA A receptor subtype selectivity underlying selective anxiolytic effect of baicalin. Neuropharmacology 2008; 55:1231–7. [PubMed: 18723037]

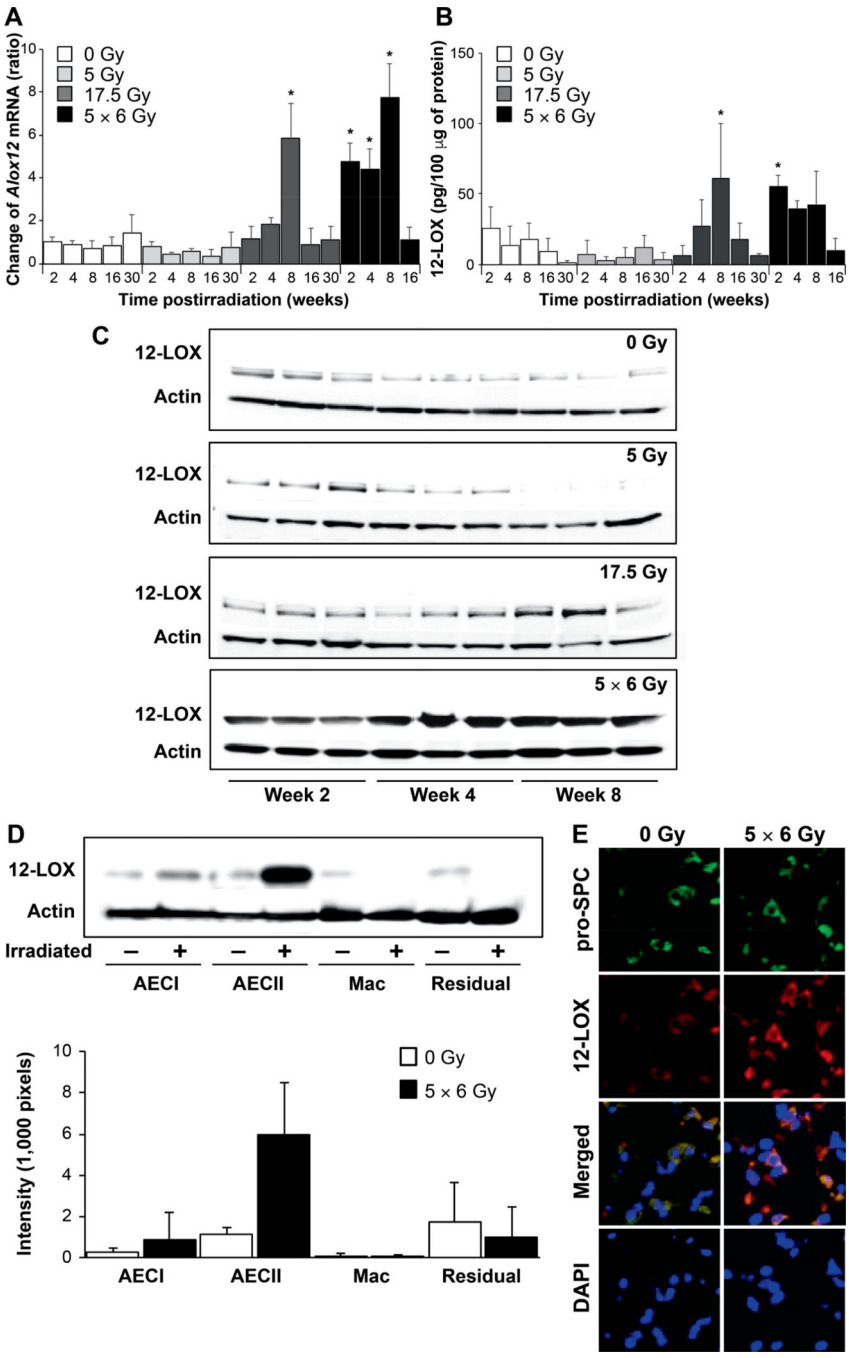

FIG. 1.

Increased expression of 12-LOX in irradiated lungs. C57/Bl6NcR mice, 8–10 weeks old, received thoracic irradiation (0 Gy, 5 Gy, 17.5 Gy or 5 × 6 Gy) and maintained for 2, 4, 6, 8, 16 or 30 weeks. Lung tissue was collected at the indicated timepoints. Panel A: RNA was isolated from lung tissue at expsoure and timepoints noted (n = 3 mice per condition). The expression of *Alox12* was determined using RT-PCR and normalized to β-actin. The normalized expression of *Alox12* is presented relative to 0 Gy, week 2. Panel B: The concentration of 12-LOX in homogenized lung tissue was determined with ELISA at the

indicated timepoints postirradiation. Panel C: Protein expression of 12-LOX in irradiated lung tissue was confirmed by Western blotting of lung tissue lysates. Panel D: Lung tissue from mice that received thoracic irradiation at varying doses was digested to a single cell suspension and macrophage, pneumocyte and remaining cell populations were enriched for analysis. The expression of 12-LOX was determined in protein lysates from enriched cell populations (n = 3); representative blot shown. Densitometry was used to quantitatively represent differences in 12-LOX expression relative to actin. Panel E: Lung tissue collected at 8 weeks postirradiation was subjected to immunofluorescence to localize 12-LOX expression relative to that of prosurfactant-C, a marker of type 2 pneumocytes. Columns are the mean and bars represent standard deviation (SD), $*P < 0.05$ compared to 0 Gy, week 2 by ANOVA. Mac = macrophages; residual = residual digested lung cellular content after AECI, AECII and macrophages removed. pro-SPC = pro-surfactant C.

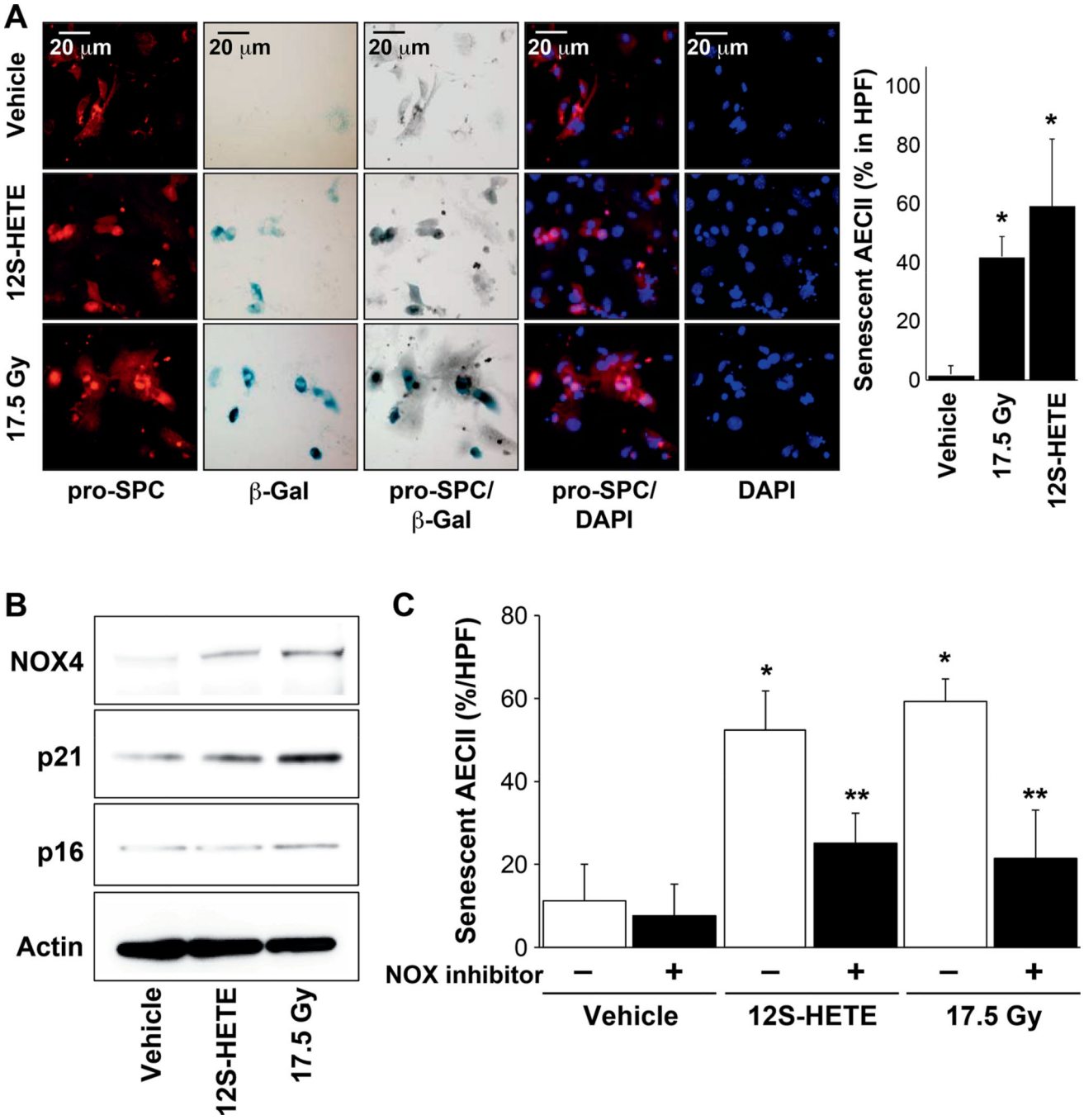

FIG. 2.

12S-HETE exposure induces senescence in AECII. Primary AECII were enriched from 8–10-week-old C57/Bl6NcR mice and cultured in chamber slides. AECII cultures received 17.5 Gy irradiation or treated with 150 n*M* 12S-HETE for 3 days. Panel A: Senescence was assessed using SA-β-galactosidase activity assay and followed by immunocytochemical localization of pro-surfactant C. The percentage of senescent AECII was scored. Columns are the mean and bars represent SD, $*P < 0.05$ relative to vehicle. Panel B: Protein lysates were prepared from enriched primary AECII cultures and subjected to Western blotting.

Panel C: Enriched primary AECII cultures were treated with 150 nM 12S-HETE or irradiated at 17.5 Gy. NOX inhibitor, 150 n*M* GKT137831 or vehicle (DMSO) was added 1 h prior to irradiation or 12S-HETE administration. After 3 days, β-galactosidase activity was determined followed by immunofluorescence for pro-surfactant C. The percentage of AECII with SA-β-gal activity was scored. Columns are the mean and bars represent SD, *$P < 0.05$ to untreated vehicle by ANOVA with Tukey's correction; **$P < 0.05$ to the corresponding treated control (vehicle, 12S-HETE, 17.5 Gy) without NOX4 inhibitor by ANOVA with Tukey's correction.

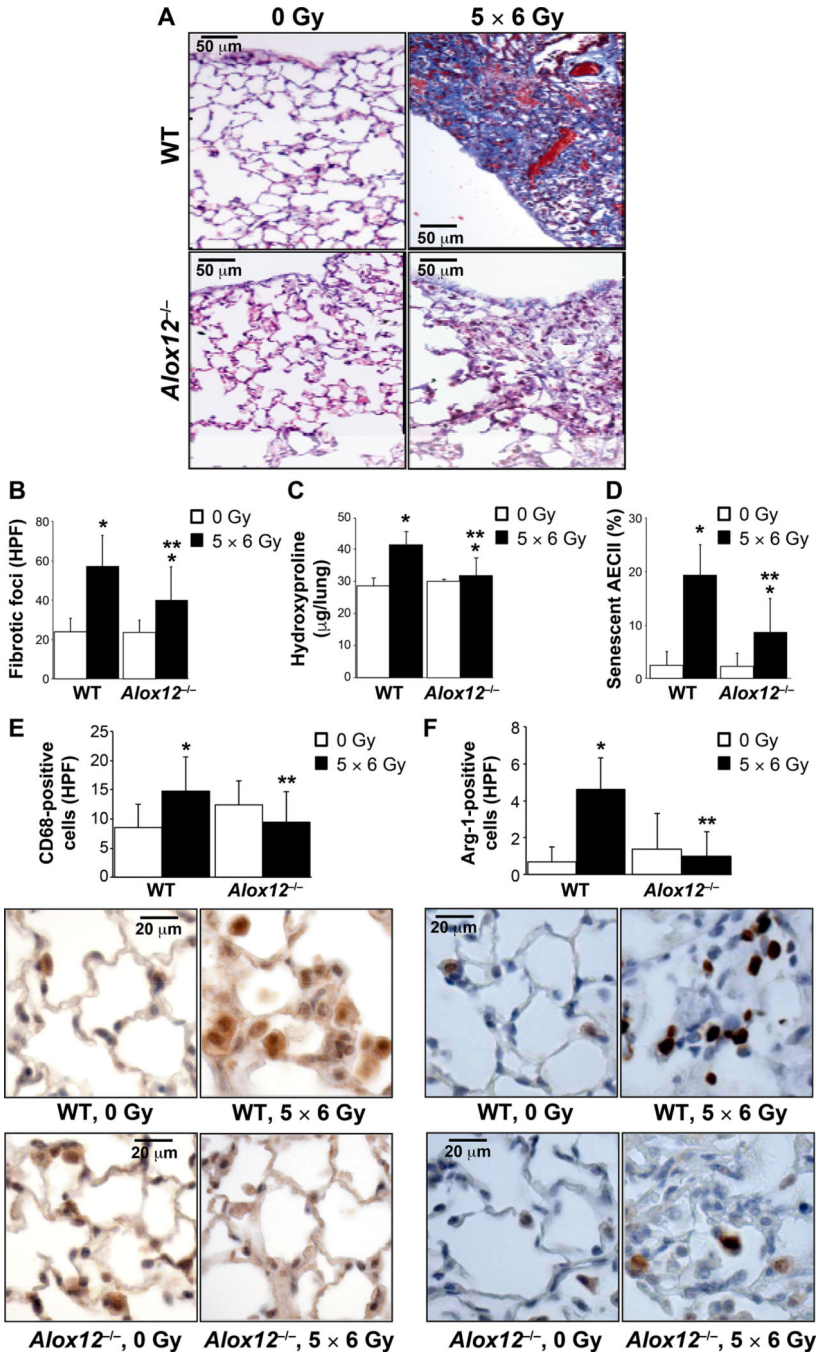

FIG. 3.

12-LOX deficiency reduces lung fibrosis after thoracic irradiation. Wild-type mice (WT) or 12-LOX-deficient mice (*Alox12*$^{-/-}$) were subjected to 5 × 6 Gy thoracic irradiation and followed until tissue collection at 16 weeks postirradiation (n = 5). Panel A: Lung sections collected at 16 weeks postirradiation were subjected to Masson's trichrome staining (collagen: light blue; epithelia: red; nuclei: dark blue). Dense fibrotic foci are evident in irradiated (5 × 6 Gy) wild-type mice but are markedly reduced in the lungs of similarly treated *Alox12*$^{-/-}$ mice. Panel B: The number of fibrotic foci per lung was assessed using

Masson's trichrome stained specimens. Panels C and D: Hydroxyproline content and percentage of AECII with senescence-associated β-galactosidase activity, respectively were assessed in lung tissue. Lung sections from the 16-week timepoint were immunostained for (panel E) CD68 and (panel F) *arginase-1*, and counterstained with hematoxylin (blue). Representative high-power images are presented. Columns are the mean and bars represent SD, $*P < 0.05$ to isogenic untreated control by ANOVA with Tukey's correction. $**P < 0.05$ for comparison to radiated wild-type by ANOVA with Tukey's correction.

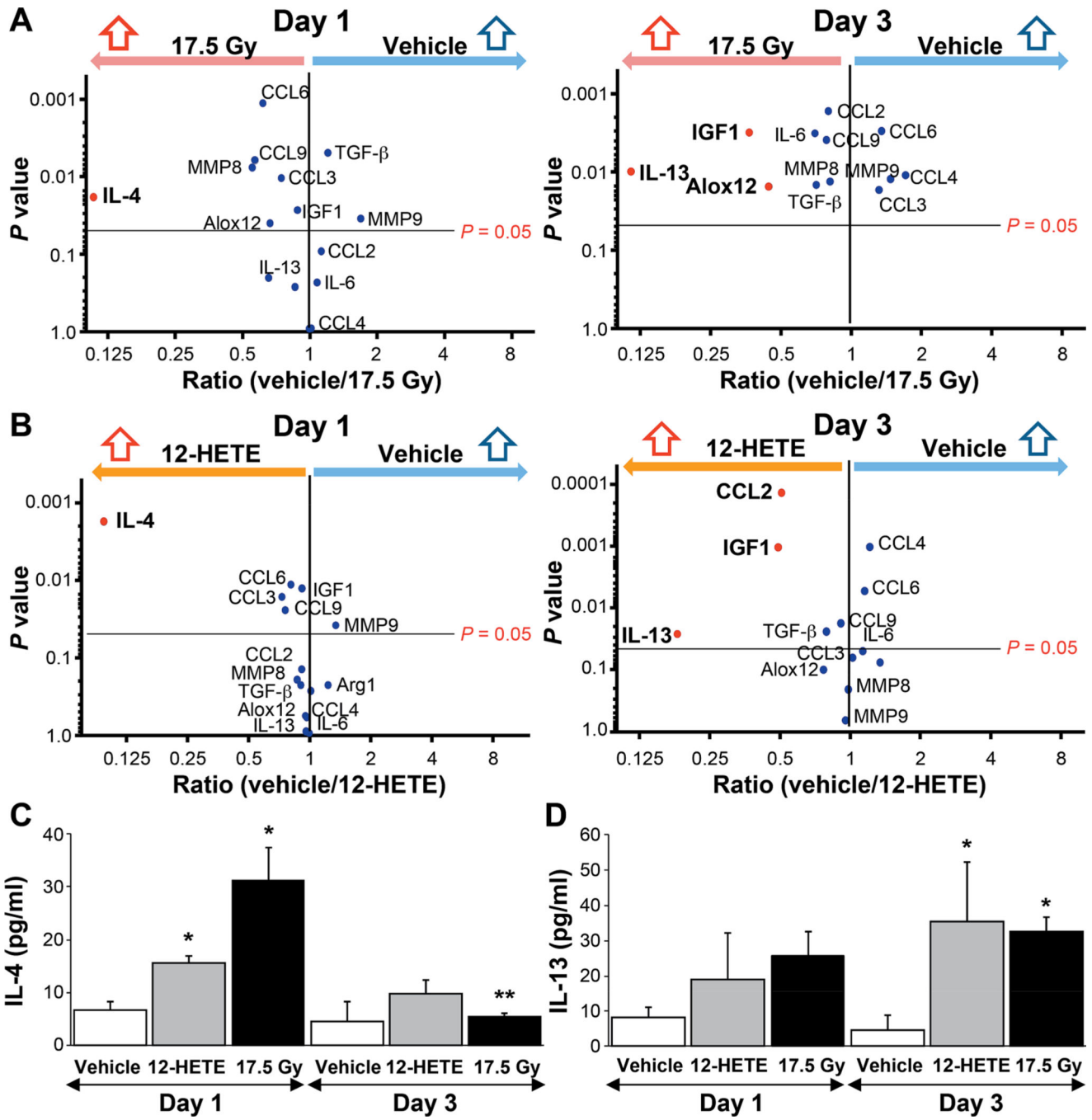

FIG. 4.

Radiation and 12S-HETE exposure increase the expression of IL-4 and IL-13 in primary AECII cultures. Enriched primary AECII cultures either 17.5 Gy irradiated (panel A) or administered 150 nM 12S-HETE (panel B) and maintained for 1 or 3 days. RNA was isolated from treated AECII cultures and the expression of several genes previously implicated in lung fibrosis were assessed and normalized to β-actin. Panels C and D: Enriched primary AECII cultures were either treated with 150 n*M* 12S-HETE or irradiated at 17.5 Gy for 1 or 3 days, and cells were then maintained in 0.5% FBS, reduced serum

media for 16 h. Conditioned media was collected and subjected to ELISA for IL-4 and IL-13. Columns are the mean and bars represent SD. *$P < 0.05$ compared to vehicle within timepoint by ANOVA. **$P < 0.05$ compared to same treatment across days 1 to 3 by ANOVA.

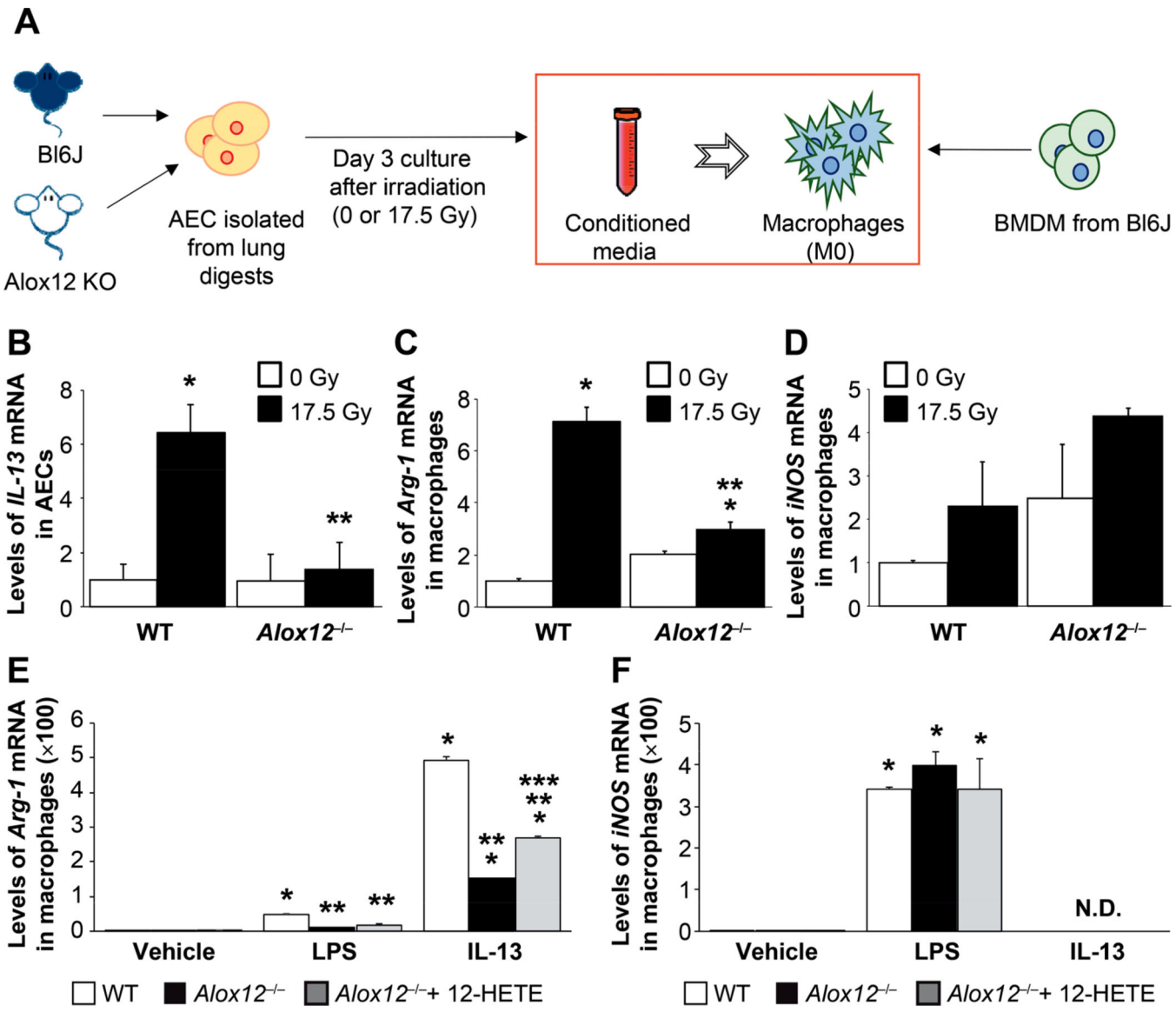

FIG. 5.

Factors secreted by AECII after irradiation can alter macrophage polarization in a 12-LOX dependent fashion. Panel A: Primary AECII cultures were generated from lung digests of wild-type (WT) or 12-LOX-deficient mice (*Alox12*$^{-/-}$) and *in vitro* irradiated (0 Gy or 17.5 Gy). Conditioned media from irradiated AECII cultures was applied to wild-type bone marrow-derived monocytes (BMDM). Panel B: *IL-13* mRNA expression in AECII cultures from wild-type and *Alox12*$^{-/-}$ mice was determined with RT-PCR. Panels C and D: BMDM from wild-type mice were treated with conditioned media from irradiated wild-type or *Alox12*$^{-/-}$ pneumocyte cultures. After 24 h of exposure to conditioned media, RNA from macrophages was isolated and the expression of *arginase-1* and *iNOS* was assessed. Columns are the mean and bars represent SD. *$P < 0.05$ for comparison to isogenic control (0 Gy) by ANOVA. **$P < 0.05$ for comparison to irradiated wild-type by ANOVA. Panels E and F: BMDM from wild-type and *Alox12*$^{-/-}$mice were treated with vehicle, LPS, IL-13 or

12S-HETE. After 24 h of exposure, RNA from macrophages was isolated and the expression of *arginase-1* and *iNOS* was assessed. Columns are the mean and bars represent SD. *$P <$ 0.05 for the comparison to wild-type vehicle by ANOVA. **$P < 0.05$ for the comparison to wild-type within each treatment group by ANOVA. ***$P < 0.05$ for the comparison to *Alox12*$^{-/-}$ within a treatment group by ANOVA.